Slug Flow Heat Transfer with Mass Injection and Linearly Varying Wall Temperature

W. S. YU and JOHN C. CHEN
Brookhaven National Laboratory, Upton, New York

The purpose of this study was to determine the two-dimensional temperature field for a fluid in slug flow through tubes with uniform mass injection and linearly decreasing wall temperature. A series solution was obtained, the first ten eigenvalues for which were determined from the characteristic equation by the method of Runge-Kutta. Expressions for local conductive heat flux at the tube wall and local Nusselt number were obtained as a function of inlet Peclet number, injection Peclet number, tube radius, temperature boundary conditions, and fluid properties. Sample results are presented for several injection rates at different wall temperature conditions. In general, mass injection was found to decrease the local heat flux and increase temperature driving force causing a decrease in the Nusselt number.

Convective heat transfer with mass injection has been treated in two classes of problems: external boundary-layer flows over plates, cylinders, etc. (*1* to *3*), and internal flows through channels (*4* to *9*). The problem considered in this study is of the second class. Among previous works in this field are those of Yuan and co-workers, who made major contributions in obtaining solutions for flow in pipes with coolant injection through porous walls for both laminar flow (*4* to *6*) and turbulent flow (*7* to *9*). Terrill recently published the solution for laminar flow between parallel plates with either mass injection or suction (*10*).

In all these studies the wall temperature of the pipe was assumed to undergo a step change at the inlet and to remain *constant* thereafter. In the present study, interest was centered on the effect of a linearly *varying* wall temperature on radial and axial temperature profiles and on heat transfer coefficients for flow through pipes with mass addition at the local wall temperature. The results of this study find application in such problems as transpiration cooling and nonequilibrium two-phase flow (*11*).

Specifically, the problem considered is defined as follows: (1) slug flow through circular pipe, (2) uniform mass injection in region $x \geq 0$, (3) uniform inlet temperature T_o at $x = 0$, (4) wall temperature varies as $T_w = T_s - B\frac{x}{r_w}$ for $x \geq 0$, (5) mass injected at wall is of same kind as in main stream, (6) injected mass is at local wall temperature, (7) constant physical properties, (8) negligible axial heat conduction, and (9) steady state.

ANALYSIS

In terms of the coordinate system shown in Figure 1, the axial velocity at position x for the conditions defined above is

$$u(x) = u_o - 2v_w\frac{x}{r_w} \tag{1}$$

where u_o is the inlet velocity and v_w is the injection velocity at wall. For steady state slug flow and constant physical properties, the continuity equation then requires the radial velocity to be

$$v(r) = v_w\frac{r}{r_w} \tag{2}$$

The energy transport equation, with axial conduction and viscous dissipation neglected, is

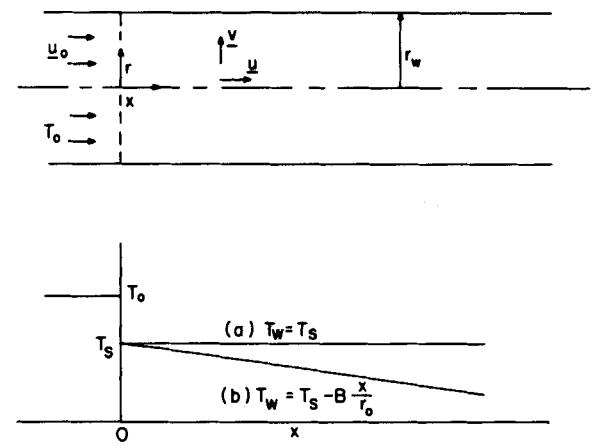

Fig. 1. Coordinate system and wall temperature profiles.

$$\rho u C_p \frac{\partial T}{\partial x} + \rho v C_p \frac{\partial T}{\partial r} = \frac{k}{r}\frac{\partial}{\partial r}\left(r\frac{\partial T}{\partial r}\right) \tag{3}$$

Using Equations (1) and (2), one can rewrite this equation

$$\frac{\partial^2 T}{\partial r^2} + \left(\frac{1}{r} - \frac{\rho C_p}{k}\frac{v_w}{r_w}r\right)\frac{\partial T}{\partial r} - \frac{\rho C_p}{k}\left(u_o - 2v_w\frac{x}{r_w}\right)\frac{\partial T}{\partial x} = 0 \tag{4}$$

Defining the dimensionless temperature

$$\theta(x, r) = \frac{T(x, r) - T_s}{T_o - T_s} \tag{5}$$

one can express Equation (4) in terms of dimensionless variables as

$$\frac{\partial^2\theta}{\partial\xi^2} + \left(\frac{1}{\xi} - \frac{N_{Pe_w}}{2}\xi\right)\frac{\partial\theta}{\partial\xi} - \left(\frac{N_{Pe_o}}{2} - N_{Pe_w}\eta\right)\frac{\partial\theta}{\partial\eta} = 0 \tag{6}$$

where

$$N_{Pe_o} = 2\frac{\rho C_p}{k} r_w u_o$$
$$N_{Pe_w} = 2\frac{\rho C_p}{k} r_w v_w \tag{7}$$

The boundary conditions are

$$\theta(\eta = 0, \xi) = 1 \tag{8}$$

$$\left.\frac{\partial\theta}{\partial\xi}\right]_{\xi=0} = 0 \tag{9}$$

$$\theta(\eta, \xi = 1) = -\left(\frac{B}{T_o - T_s}\right)\eta = -\beta\eta \tag{10}$$

The above system of equations defines the temperature field as a function of position, the two Peclet parameters N_{Pe_o} and N_{Pe_w} and the boundary temperature parameter $\beta = B/(T_o - T_s)$. The problem is solved first for the case of a step change in wall temperature ($\beta = 0$) and then for the more general case of a linearly varying T_w.

Step Change in T_w

By separation of variables

$$\theta(\eta, \xi) = X(\eta)\cdot R(\xi) \tag{11}$$

Then Equation (6) yields the ordinary differential equations

$$R''(\xi) + \left(\frac{1}{\xi} - \frac{1}{2}N_{Pe_w}\xi\right)R'(\xi) + \lambda^2 R(\xi) = 0 \tag{12}$$

$$\left(\frac{1}{2}N_{Pe_o} - N_{Pe_w}\eta\right)X'(\eta) + \lambda^2 X(\eta) = 0 \tag{13}$$

Equation (13) can be integrated directly to obtain

$$X(\eta) = C\left(1 - 2\frac{N_{Pe_w}}{N_{Pe_o}}\eta\right)^{\lambda^2/N_{Pe_w}} \tag{14}$$

Since the Sturm-Louville requirements are satisfied, the solution for $\theta(\eta, \xi)$ may be expressed as an orthogonal series:

$$\theta(\eta, \xi) = \sum_n A_n\cdot X_n(\eta)\cdot R_n(\xi) \tag{15}$$

The series coefficients A_n may be evaluated by means of boundary condition (8):

$$\text{at } \eta = 0,\ \theta(\eta = 0, \xi) = 1$$
$$1 = \sum_n A_n\cdot R_n(\xi)$$

where

$$A_n = \frac{\int_0^1 \phi(\xi)\cdot R_n(\xi)\,d\xi}{\int_0^1 \phi(\xi)\cdot R_n^2(\xi)\,d\xi} \tag{16}$$

The weighting function $\phi(\xi)$ is obtained from Equation (12).

$$\phi(\xi) = \exp\left[\int\left(\frac{1}{\xi} - \frac{1}{2}N_{Pe_w}\xi\right)d\xi\right]$$
$$= \xi\cdot\exp\left(-N_{Pe_w}\xi^2/4\right) \tag{17}$$

Therefore

$$A_n = \frac{\int_0^1 \xi\cdot R_n(\xi)\cdot e^{-N_{Pe_w}\xi^2/4}\,d\xi}{\int_0^1 \xi\cdot R_n^2(\xi)\cdot e^{-N_{Pe_w}\xi^2/4}\,d\xi} \tag{18}$$

The solution for the temperature distribution is then

$$\theta(\eta, \xi) = \sum_n A_n\left(1 - 2\frac{N_{Pe_w}}{N_{Pe_o}}\eta\right)^{\lambda_n^2/N_{Pe_w}}\cdot R_n(\xi) \tag{19}$$

The eigenvalues λ_n and eigenfunctions $R_n(\xi)$ are to be evaluated from the characteristic Equation (12) together with boundary conditions (9) and (10).

The conductive heat transfer at the wall is

$$Q(\eta) = -\frac{k}{r_w}(T_o - T_s)\left(\frac{\partial\theta}{\partial\xi}\right)_{\xi=1}$$
$$= -\frac{k}{r_w}(T_o - T_s)\sum_n A_n\left(1 - 2\frac{N_{Pe_w}}{N_{Pe_o}}\right)^{\lambda_n^2/N_{Pe_w}}\cdot R_n'(1) \tag{20}$$

from which the local Nusselt number is obtained as

$$N_{Nu}(\eta) = \frac{2r_w Q(\eta)}{k(T_b - T_w)}$$

$$N_{Nu}(\eta) = \frac{-\sum_n A_n\left(1 - 2\frac{N_{Pe_w}}{N_{Pe_o}}\eta\right)^{\lambda_n^2/N_{Pe_w}}\cdot R_n'(1)}{\sum_n A_n\left(1 - 2\frac{N_{Pe_w}}{N_{Pe_o}}\eta\right)^{\lambda_n^2/N_{Pe_w}}\cdot\int_0^1 R_n(\xi)\cdot\xi\,d\xi} \tag{21}$$

Linearly Varying T_w

For wall temperature varying as a linear function of x, boundary condition (10) applies with $\beta \neq 0$. It is necessary to introduce the following transformation of the axial coordinate variable:

$$\chi = -\frac{1}{N_{Pe_w}}\ln\left(1 - \frac{2N_{Pe_w}}{N_{Pe_o}}\eta\right) \tag{22}$$

Equation (6) may then be written as

$$\frac{\partial^2\theta}{\partial\xi^2} + \left(\frac{1}{\xi} - \frac{N_{Pe_w}}{2}\xi\right)\frac{\partial\theta}{\partial\xi} - \left(\frac{N_{Pe_o}}{2} - N_{Pe_w}\eta\right)\frac{\partial\theta}{\partial\chi}\cdot\frac{\partial\chi}{\partial\eta} = 0$$
$$\frac{\partial^2\theta}{\partial\xi^2} + \left(\frac{1}{\xi} - \frac{N_{Pe_w}}{2}\xi\right)\frac{\partial\theta}{\partial\xi} - \frac{\partial\theta}{\partial\chi} = 0 \tag{23}$$

so that the requirement for a constant coefficient on the axial term is satisfied. The stepwise temperature solution, Equation (19), is then

TABLE 1. EIGENVALUES, SERIES COEFFICIENTS, AND DERIVATIVES OF EIGENFUNCTION

	$N_{Pe_w}=-1$			$N_{Pe_w}=-2$			$N_{Pe_w}=-6$			$N_{Pe_w}=-10$		
n	λ_n^2	A_n	$R_n'(1)$	λ_n^2	A_n	$R_n'(1)$	λ_n^2	A_n	$R_n'(1)$	λ_n^2	A_n	$R_n'(1)$
1	6.29681	1.6663	−1.0998	6.83762	1.7359	−0.96532	9.26756	2.0732	−0.55286	12.0988	2.5172	−0.29940
2	30.9907	−1.1860	1.6570	31.5492	−1.3189	1.4608	34.1738	−1.9881	0.87619	37.4307	−2.9321	0.51916
3	75.4073	0.95758	−2.0728	75.9681	1.0771	−1.8284	78.6182	1.7087	−1.1040	81.9237	2.6798	−0.66351
4	139.561	−0.82365	2.4188	140.122	−0.92938	2.1341	142.780	−1.5002	1.2913	146.099	−2.4058	0.77939
5	223.453	0.73313	−2.7214	224.015	0.82854	−2.4013	226.676	1.3480	−1.4543	230.001	2.1838	−0.87941
6	327.084	−0.66696	2.9937	327.646	−0.75439	2.6417	330.309	−1.2325	1.6006	333.637	−2.0077	0.96884
7	450.455	0.61591	−3.2433	451.017	0.69700	−2.8620	453.681	1.1416	−1.7346	457.010	1.8657	−1.0505
8	593.564	−0.57501	3.4750	594.127	−0.65092	3.0666	596.791	−1.0678	1.8589	600.121	−1.7488	1.1262
9	756.414	0.54128	−3.6923	756.976	0.61287	−3.2583	759.641	1.0065	−1.9754	762.972	1.6507	−1.1971
10	939.003	−0.51286	3.8974	939.565	−0.58078	3.4394	942.231	−0.95450	2.0853	945.562	−1.5670	1.2639

$$\theta(\chi,\xi)=\sum_n A_n\left(e^{-\lambda_n^2\chi}\right)\cdot R_n(\xi) \tag{24}$$

Next, define

$$\theta^*=1-\theta \tag{25}$$

so that

$$\theta^*(\chi=0,\ \xi\neq 1)=0 \tag{26}$$

$$\theta^*(\chi,\ \xi=1)=1+\frac{\beta N_{Pe_o}}{2N_{Pe_w}}\left(1-e^{-N_{Pe_x}\chi}\right) \tag{27}$$

Applying Duhamel's superposition theorem, we get

$$\theta^*(\chi,\xi)=[1-\theta(\chi=0,\ \xi=1)]\cdot[1-\theta(\chi,\xi)]-\int_0^\chi[1-\theta(\chi-\tau,\xi)]\cdot\frac{\partial}{\partial\chi}\theta(\tau,\ \xi=1)\ d\tau \tag{28}$$

where θ is the temperature distribution due to an incremental step change in wall temperature, as given by Equation (24). Substituting Equation (24) into Equation (28) and applying boundary conditions (26, 27), we get

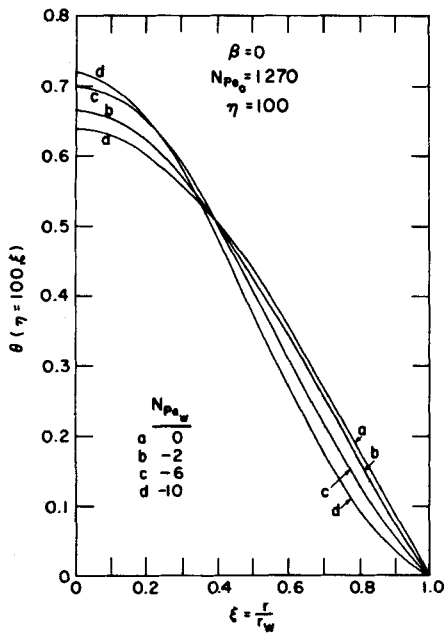

Fig. 2. Radial temperature profiles at different mass injection rates.

$$\theta^*(\chi,\xi)=1-\sum_n A_n e^{-\lambda_n^2\chi}\cdot R_n(\xi)-\frac{\beta N_{Pe_o}}{2}\times\int_0^\chi\left[1-\sum_n A_n e^{-\lambda_n^2(\chi-\tau)}\cdot R_n(\xi)\right]e^{-NPe_w\tau}\,d\tau \tag{29}$$

After evaluation of the integral and transformation to the η coordinate, we obtain the solution for the temperature distribution as

$$\theta(\eta,\xi)=\sum_n A_n\left(1-2\frac{N_{Pe_w}}{N_{Pe_o}}\eta\right)^{\lambda_n^2/NPe_w}\cdot R_n(\xi)-\beta\eta-\frac{\beta N_{Pe_o}}{2N_{Pe_w}}\sum_n\frac{A_n N_{Pe_w}}{N_{Pe_w}-\lambda_n^2}\left[1-\frac{2N_{Pe_w}}{N_{Pe_o}}\eta-\left(1-\frac{2N_{Pe_w}}{N_{Pe_o}}\eta\right)^{\lambda_n^2/NPe_w}\right]\times R_n(\xi) \tag{30}$$

The expression is seen to reduce to Equation (19) for special case of a step-change wall temperature ($\beta=0$). For the degenerate case of $N_{Pe_w}=0$, the solution for the temperature field was obtained as

$$\theta(\eta,\xi)=-\beta\eta+\frac{\beta N_{Pe_o}(1-\xi^2)}{8}+\sum_n\frac{2}{\alpha_n J_1(\alpha_n)}J_0(\alpha_n\xi)\,e^{-2\alpha_n^2\eta/NPe_o}-\frac{\beta N_{Pe_o}}{2}\sum_n\frac{2}{\alpha_n^3 J_1(\alpha_n)}J_0(\alpha_n\xi)\,e^{-2\alpha_n^2\eta/NPe_o} \tag{31}$$

where J_0 and J_1 are Bessel's functions of orders zero and one, and α_n are the roots of J_0.

For the general case, the conductive heat transfer at the wall is

$$Q(\eta)=-\frac{k}{r_w}(T_o-T_s)\sum_n A_n\left(1-2\frac{N_{Pe_w}}{N_{Pe_o}}\eta\right)^{\lambda_n^2/NPe_w}R_n'(1)+\beta(T_o-T_s)\frac{k}{r_w}\left(\frac{N_{Pe_o}}{2N_{Pe_w}}\right)\sum_n\frac{A_n N_{Pe_w}}{N_{Pe_w}-\lambda_n^2}\times\left[1-\frac{2N_{Pe_w}}{N_{Pe_o}}\eta-\left(1-\frac{2N_{Pe_w}}{N_{Pe_o}}\eta\right)^{\lambda_n^2/NPe_w}\right]\cdot R_n'(1) \tag{32}$$

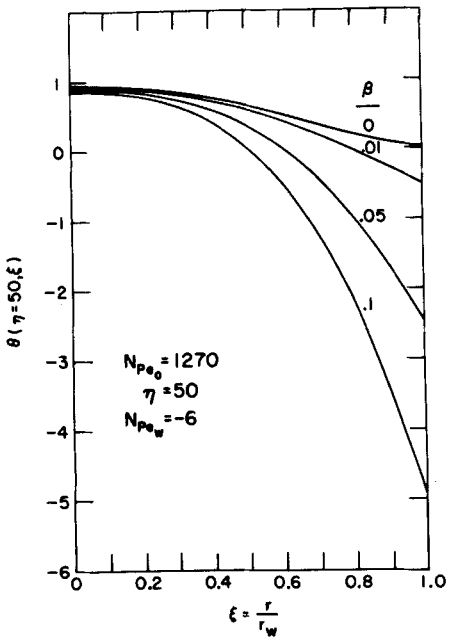

Fig. 3. Radial temperature profiles at different boundary temperature conditions.

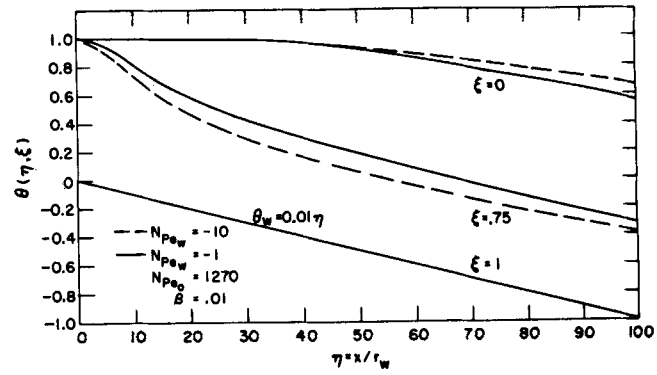

Fig. 4. Axial temperature profiles for two different mass injection rates.

and the local Nusselt number is determined to be

$$N_{Nu}(\eta) = \frac{-2}{\beta\eta + 2\int_0^1 \theta(\eta,\xi)\cdot\xi\, d\xi}\cdot\left(\frac{\partial\theta}{\partial\xi}\right)_{\xi=1}$$

$$N_{Nu}(\eta) = -\sum_n A_n \cdot R_n'(1)\cdot\left\{\left(1-\frac{2N_{Pe_w}}{N_{Pe_o}}\right)\eta^{\lambda_n^2/N_{Pe_w}} - \frac{\beta N_{Pe_o}}{2(N_{Pe_w}-\lambda_n^2)}\left[1-\frac{2N_{Pe_w}}{N_{Pe_o}}\eta-\left(1-\frac{2N_{Pe_w}}{N_{Pe_o}}\eta\right)^{\lambda_n^2/N_{Pe_w}}\right]\right\}\Bigg/$$

$$\sum A_n\cdot\left\{\left(1-\frac{2N_{Pe_w}}{N_{Pe_o}}\eta\right)^{\lambda_n^2/N_{Pe_w}} - \frac{\beta N_{Pe_o}}{2(N_{Pe_w}-\lambda_n^2)}\left[1-\frac{2N_{Pe_w}}{N_{Pe_o}}\eta-\left(1-\frac{2N_{Pe_w}}{N_{Pe_o}}\eta\right)^{\lambda_n^2/N_{Pe_w}}\right]\right\}\cdot\int_0^1 R_n(\xi)\cdot\xi\, d\xi \quad (33)$$

RESULTS AND DISCUSSION

To obtain numerical results, one must first determine the eigenvalues λ_n and the eigenfunctions $R_n(\xi)$. Unfortunately, the characteristic Equation (12) is a confluent hypergeometric differential equation for which no usable explicit solution is available. In this study, Equation (12) was solved numerically by the method of Runge-Kutta on a digital computer. A trial and error procedure was employed to obtain values for λ_n and $R_n(\xi)$ such that boundary conditions (9) and (10) are satisfied.* While this is a lengthy process, it does enable the eigenconstants to be determined to as high a degree of accuracy as desired.

The eigenvalues λ_n, eigenfunctions $R_n(\xi)$, and expansion coefficients A_n are functions only of the mass injection Peclet number N_{Pe_w}. Values of these quantities, for the first ten terms of the series in Equation (19) (first ten eigenvalues), were computed for four cases:

$$N_{Pe_w} = -1, -2, -6, -10$$

Negative N_{Pe_w} denotes mass addition to the stream. The results obtained for λ_n, A_n, and $R_n'(1)$ are presented in Table 1. We believe that values for λ_n and A_n are accurate to six and five significant figures, respectively.

Using these eigenvalues and the corresponding eigenfunctions, one can determine both radial and axial temperature profiles from Equation (30) for any desired entrance Peclet number N_{Pe_o}, any linear wall temperature variation (as denoted by the value of β) at different mass injection rates (as denoted by N_{Pe_w}). Figure 2 shows examples of the radial temperature profiles calculated by Equation (30) for different mass injection rates at a position 50 diameters from the entrance, for the case of $\beta = 0$. It is seem that mass injection tends to decrease the local temperatures in the vicinity of the wall while increasing the temperatures near the center line. The first effect follows from the lowering of local mixed temperatures near the wall by the addition of the colder injected mass which enters the stream at the wall temperature. The second effect is caused by the increase of bulk axial velocity due to mass addition inasmuch as this increased velocity allows less residence time for cooling of the fluid. The second effect would be most noticeable at the point furthest from the cold sink, that is, at the center line.

Figure 3 shows radial temperature profiles calculated by

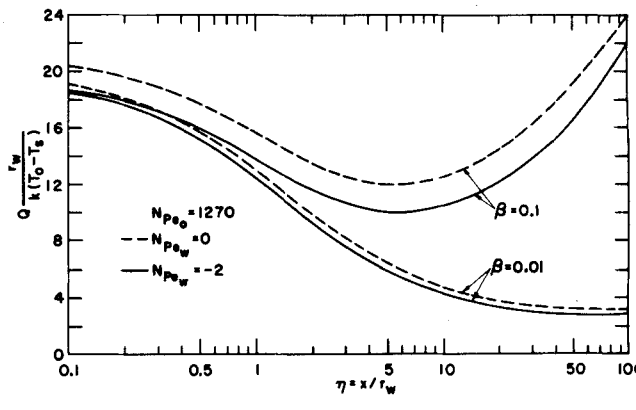

Fig. 5. Conductive heat flux at wall.

*This technique for obtaining eigenvalues has been used previously by Hsu (12) and Yuan and Peng (5).

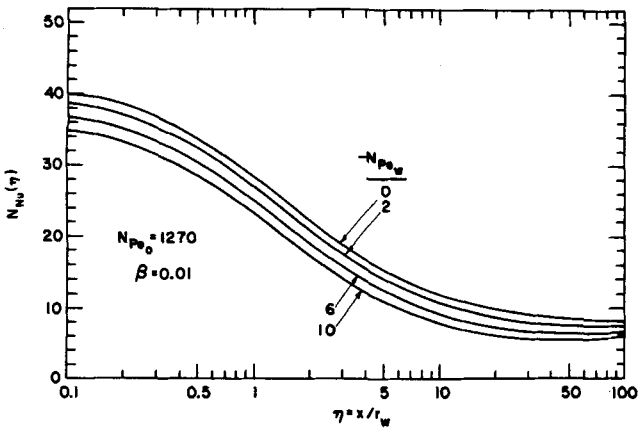

Fig. 6. Local Nusselt numbers for different mass injection rates.

Equation (30) for one injection rate at various wall temperature conditions. As expected, more steeply decreasing wall temperatures (increasing values of β) result in steeper gradients throughout the temperature field with maximum effect at the wall and minimum effect near the center line. It also overcomes the tendency for S-shaped profiles caused by cold mass addition, giving radial profiles of the more normal parabolic shape.

Examples of axial temperature profiles calculated from Equation (30) are shown in Figure 4. Results plotted are for $\beta = 0.01$ at two different mass injection rates ($N_{Pe_w} = -1, -10$). As noted above, increased mass addition decreases $(-\partial\theta/\partial\eta)$ for $\xi \longrightarrow 0$ and increases it for $\xi \longrightarrow 1$. The net result is that the temperature drop from center line to wall increases with increasing $(-N_{Pe_w})$ and increasing η.

The effect of varying boundary conditions on conductive heat flux at the wall, with and without mass injection, is illustrated in Figure 5. At a low value of β the heat flux is seen to decrease in the normal fashion along the axis, exhibiting the usual entrance region effect. At a high value of β the heat flux first decreases as the effect of the initial step change in wall temperature diminishes; but then the flux reaches a minimum and increases again—reflecting the steeper radial temperature profiles which result from the continuously decreasing wall temperature. The results also show that mass injection decreases the local conductive heat flux, the decrease being greater at high values of β.

Local Nusselt numbers calculated from Equation (33) are plotted in Figure 6 for several different rates of mass injection. Increasing injection decreases the heat flux and increases the temperature driving force, so that there is a reduction in local Nusselt number as mass injection is increased.

SUMMARY

A general solution for the temperature field of a fluid in slug flow through tubes, with mass injection and linearly decreasing wall temperatures, was obtained in terms of an orthogonal series. The first ten eigenvalues and eigenfunctions were determined by numerical solution of the characteristic equation. Calculated results indicated that radial temperature profiles change from the normal parabolic shape to an S shape as mass injection increases, and temperature difference from center line to wall increases with increasing mass injection. Expressions were also derived for local conductive heat flux at the wall and local Nusselt number. In general, mass injection was found to decrease the heat flux and increase the temperature driving force, causing a reduction in Nusselt number.

ACKNOWLEDGMENT

The authors express their appreciation to Dr. C. J. Hsu of Brookhaven National Laboratory and to Dr. Ralph Stein of Argonne National Laboratory for pertinent and helpful suggestions during the course of this study. This work was performed under the auspices of the U. S. Atomic Energy Commission.

NOTATION

A_n = coefficients of series expansion in Equation (19)
B = constant, slope of wall temperature gradient
C = integration constant
C_p = specific heat, B.t.u./(lb.$_m$)(°F.)
J = Bessel's function
k = thermal conductivity, B.t.u./(hr.)(ft.)(°F.)
N_{Nu} = $2r_w h/k$, Nusselt number, dimensionless
N_{Pe} = Peclet number defined by Equation (7), dimensionless
Q = heat flux, B.t.u./(hr.)(sq. ft.)
r = radius, ft.
R = eigenfunction of Equation (12)
T = local fluid temperature, °F.
T_s = wall temperature at inlet, °F.
u = axial velocity, ft./sec.
v = radial velocity, ft./sec.
x = axial distance, ft.
X = defined by Equation (13)

Greek Letters

α = root of zero-order Bessel's function
$\beta = B/(T_o - T_s)$
$\eta = x/r_w$, dimensionless axial distance
$\theta = (T - T_s)/(T_o - T_s)$, dimensionless local temperature
$\theta^* = 1 - \theta$
λ = eigenvalue of Equations (12) and (13)
$\xi = r/r_w$, dimensionless radial distance
ρ = density, lb./cu. ft.
χ = defined by Equation (22)
τ = defined by Equation (28)
ϕ = weighting function, defined by Equation (17)

Subscripts

o = inlet
b = bulk
w = wall
n = index

LITERATURE CITED

1. Brown, W. B., and P. L. Donoughe, *Natl. Advisory Comm. Aeronaut. Tech. Note 2479* (Sept., 1951).
2. Eckert, E. R. G., *Air Material Command Tech. Rept.* 5646 (Nov., 1947).
3. Hartnett, J. P., and E. R. G. Eckert, *Trans. Am. Soc. Mech. Engrs.*, **79**, 247–254 (Feb., 1957).
4. Yuan, S. W., and A. B. Finkelstein, *Jet Propulsion*, **28**, No. 3, 178–181 (Mar., 1958).
5. Yuan, S. W., and Y. Peng, *Intern. Develop. Heat Transfer*, **4**, 717–724 (Aug., 1961).
6. Peng, Y., and S. W. Yuan, *Trans. Am. Soc. Mech. Engrs.*, **87**, 252–258 (May, 1965).
7. Yuan, S. W., and L. S. Galowin, *Proc. 9th Intern. Congr. Appl. Mech.*, **2**, 331–340 (1957).
8. Yuan, S. W., R. F. Pohler, and W. F. Walker, *Develop. Mech.*, **1**, 526–531 (1961).
9. Yuan, S. W., and A. Barazotti, *Proc. Heat Transfer Fluid Mech. Inst.*, 25–39, Stanford University Press, Stanford, Calif. (1958).
10. Terrill, R. M., *Intern. J. Heat Mass Transfer*, **8**, 1491–1497 (Dec., 1965).
11. Chen, J. C., *AIChE J.*, **11**, No. 6, 1145 (1965).
12. Hsu, C. J., *ibid.*, No. 4, 690–695 (July, 1965).

Manuscript received December 23, 1966; revision received March 20, 1967; paper accepted March 23, 1967.